A new bounding surface model for thermal cyclic behaviour

Type of manuscript: Short Communication

Authors: C. Zhou*, K. Y. Fong and C. W. W. Ng

*Corresponding author

Information of the authors

First author: Dr C. Zhou

Visiting assistant professor, Department of Civil and Environmental Engineering, The Hong Kong University of Science and Technology, Clear Water Bay, Kowloon, Hong Kong.

E-mail: czhou@connect.ust.hk

Co-author: Mr K. Y. Fong

Research student, Department of Civil and Environmental Engineering, The Hong Kong University of Science and Technology, Clear Water Bay, Kowloon, Hong Kong.

E-mail: kyfongad@connect.ust.hk

Co-author: Dr C. W. W. Ng

Chair professor, Department of Civil and Environmental Engineering, The Hong Kong University of Science and Technology, Clear Water Bay, Kowloon, Hong Kong.

E-mail: cecwwng@ust.hk

SUMMARY

To accurately predict soil volume changes under thermal cycles is of great importance for analysing the performance of many earth structures such as energy pile and energy storage system. Most of the existing thermo-mechanical models focus on soil behaviour under monotonic thermal loading only, and they are not able to capture soil volume changes under thermal cycles. In this study, a constitutive model is proposed to simulate volume changes of saturated soil subjected to cyclic heating and cooling. Two surfaces are defined and used: a bounding surface and a memory surface. The bounding surface and memory surface are mainly controlled by the preconsolidation pressure (a function of plastic volumetric strain) and the maximum stress experienced by the soil, respectively. Under thermal cycles, the distance of the two surfaces increases with an accumulation of plastic strain. By adopting the double surface concept, a new elastoplastic model is derived from an existing single bounding surface thermo-mechanical model. Comparisons between model predictions and experimental results reveal that the proposed model is able to capture soil volume changes under thermal cycles well. The plastic strain accumulates with an increase in number of thermal cycles, but at a decreasing rate, until stabilization.

KEYWORDS: constitutive relations; thermal effects; cyclic

1. INTRODUCTION

In many earth structures such as energy pile, high-speed railway embankment and energy storage system, soils are subjected to cyclic heating and cooling [1,2]. To accurately predict soil volume changes under thermal cycles is important for analysing the performance of these structures. So far, some thermo-mechanical soil models have been developed within the elastoplastic framework [3-13]. Most of these existing models, however, focus on soil behaviour under monotonic thermal loading only. Some important aspects of thermal cyclic behaviour, such as the accumulation of plastic strain under cyclic heating and cooling, cannot be captured. Only recently, Di Donna *et al.* [14] proposed a thermo-mechanical model to simulate the plastic strain accumulation of soils under thermal cycles. In their model, to improve the modelling of cyclic effects, a new nesting surface is activated at the beginning of each new thermal cycle. Additional hardening and translation rules are defined for these nesting surfaces, making the thermo-mechanical model more complex.

In the present study, the original bounding surface plasticity theory of Dafalias [15] is modified by constructing double surfaces: a bounding surface and a memory surface. New formulations are thus proposed to describe plastic modulus, the size and evolution of the two surfaces. By adopting the double surface concept, a new elastoplastic model is derived from an existing single bounding surface thermo-mechanical model [16]. An important and challenging aspect of thermo-mechanical modelling (i.e., capturing the thermal volume changes under thermal cycles) is newly incorporated. The proposed model would be useful for predicting the performance of many geostructures such as energy foundation, energy storage system and

high-speed railway embankment under cyclic heating and cooling. In this paper, model formulations, parameter calibration and model verification are presented.

2. MATHEMATICAL FORMULATIONS

In the current thermo-mechanical model developed in the triaxial stress space, soil state are defined by using three constitutive variables, including the effective mean stress (p'), deviator stress (q) as well as temperature (T). The deformation of soil is described through incremental shear strain ($d\varepsilon_s$) and incremental volumetric strain ($d\varepsilon_v$).

2.1. Double surfaces

To capture effects of thermal cycles on soil behaviour, the original bounding surface plasticity theory [15] is modified by constructing double surfaces. Figure 1 shows the two surfaces and a loading surface in the p'- q plane. The bounding surface is expressed as

$$F = \left(\frac{q}{Mp'} \right)^n + \frac{\ln\left[p' / p_0(T)\right]}{\ln r} \tag{1}$$

where n and r are soil parameters controlling the shape of bounding surface; p_0 is the preconsolidation pressure; and M is the value of critical state stress ratio (q/p'). Equation (1) is able to represent bounding surface with various shapes. For instance, equation (1) represents the yield surface of the original Cam-clay model when n and r are 1 and 2.718 respectively. More details are reported in Zhou *et al.* [8].

The loading surface is assumed to pass the current stress state and have the same shape as the bounding surface. It follows

$$F^* = \left(\frac{q}{Mp'} \right)^n + \frac{\ln\left[p' / p_l(T) \right]}{\ln r} \tag{2}$$

where p_l is a variable describing the size of the loading surface and it can be calculated from the current stress state by using equation (2) and assuming that $F^* = 0$.

The loading surface with the maximum size in the stress history is defined as memory surface. Therefore, the memory surface can be described using the following equation:

$$F_L = \left(\frac{q}{Mp'} \right)^n + \frac{\ln\left[p' / p_m(T) \right]}{\ln r} \tag{3}$$

where p_m is equal to min (p_0, the maximum p_l in the stress history).

Figure 2 shows the double surfaces in the p'- q- ΔT space, where ΔT is the difference of soil temperature (T) and a reference temperature (T_0). The evolution of $p_0(T)$ and $p_m(T)$ with a variation of soil temperature are described by using equation (20) and (21) in the appendix, respectively.

2.2. Hardening law

The memory surface passes through the maximum stress state experienced by soil specimen (denoted by Point E in Figure 1). This surface expands isotropically when the current stress state (denoted by Point A) reaches and pushes it outward. On the other hand, the bounding surface permits isotropic strain hardening. Its size is governed by preconsolidation pressure (denoted by Point F), which increases with an increase in the plastic volumetric strain. For a soil specimen subjected to monotonic loading only, the preconsolidation pressure is equal to the maximum stress experienced. Consequently, the two surfaces collapse to a single surface. For a soil specimen subjected to thermal cycles at a constant stress, the memory surface remains

unchanged after the first cycle. This is because the current stress does not exceed the maximum stress experienced along the memory surface. On the contrary, the size of the bounding surface continues to expand due to an accumulation of plastic volumetric strain under thermal cycles, but at a decreasing rate.

2.3. Mapping rule

Radial mapping rule is used to project the current stress state, which is always on the loading surface, on the double surfaces. This mapping rule is simple but yet effective for modelling soil behaviour along many stress paths [15]. Figure 1 shows some key features of the radial mapping rule. Points O (0, 0), A (p', q), B ($\bar{p}_1'$, $\bar{q}_1$) and C ($\bar{p}_2'$, $\bar{q}_2$) are the projection center, current stress state, image stress states on the memory surface and image stress states on the bounding surface, respectively. These four points lie on a straight line. Based on the relative position of these four points, three Euclidian "distances" are defined: ρ, $\bar{\rho}_1$ and $\bar{\rho}_2$, which are the lengths of OA, OB and OC respectively. The ratio of these Euclidian "distances" is related to the stress state:

$$\frac{\rho}{\bar{\rho}_2} = \frac{p'}{\bar{p}_2'} = \frac{q}{\bar{q}_2} \tag{4}$$

$$\frac{\bar{\rho}_1}{\bar{\rho}_2} = \frac{\bar{p}_1'}{\bar{p}_2'} = \frac{\bar{q}_1}{\bar{q}_2} \tag{5}$$

The above two ratios are closely related to many aspects of soil behaviour, such as the flow rule and hardening law. More details are given later in the next section.

2.4. Elastoplasticity

As illustrated by equation (10) in the appendix, both $d\varepsilon_s$ and $d\varepsilon_v$ have an elastic and a plastic

components. The incremental elastic strains are described by

$$\begin{cases} d\varepsilon_v^e = \dfrac{dp'}{K} - \alpha_s dT \\ d\varepsilon_s^e = \dfrac{dq}{3G_0} \end{cases} \tag{6}$$

where K is bulk modulus; α_s is the isotropic thermal expansion coefficient of the soil skeleton; and G_0 is elastic shear modulus.

On the other hand, the increments of plastic strains are expressed as:

$$\begin{cases} d\varepsilon_v^p = D_s \Lambda_s \\ d\varepsilon_s^p = \Lambda_s \end{cases} \tag{7}$$

where Λ_s is the non-negative loading index; and D_s is soil dilatancy which is defined as the ratio of $d\varepsilon_v^p$ to $d\varepsilon_s^p$. The value of D_s is calculated using equation (24) in the appendix. The value of Λ_s is determined from the hardening law of the bounding surface and the condition of consistency as follows:

$$\Lambda_s = \frac{1}{K_p}\left(\frac{\partial F}{\partial p'}dp' + \frac{\partial F}{\partial q}dq + \frac{\partial F}{\partial r}\frac{\partial r}{\partial T}dT + \frac{\partial F}{\partial p_0}\frac{\partial p_0}{\partial T}dT\right) \tag{8}$$

For the equation above, the four terms in the numerator are calculated by using equations (26) through (29) in the appendix. The value of the numerator is assumed to be zero if the calculated value is negative. The denominator is determined by the condition of consistency and expressed as equation (31) when soil stress state is on the bounding surface. When stress state is within the bounding surface, however, equation (31) is modified to take into account the distance between loading surface and the double surfaces as follows:

$$K_p = \frac{\upsilon}{(\lambda-\kappa)\ln r}\frac{\left((M\bar{\rho}_2/\rho)^2(\bar{\rho}_2/\bar{\rho}_1)^{n_c}-\eta^2\right)}{2\eta} \tag{9}$$

where n_c is a soil parameter which considers the influence of cyclic effects. The factors $\bar{\rho}_2/\rho$ and $\bar{\rho}_2/\bar{\rho}_1$ are introduced in equation (9) to simulate a decrease of K_p as soil stress state moves towards the bounding surfaces. When soil stress state reaches the two bounding surfaces (at normally consolidated state) under monotonic loading, both ratios $\bar{\rho}_2/\rho$ and $\bar{\rho}_2/\bar{\rho}_1$ are equal to one and hence equation (9) reduces to equation (31).

The rate constitutive equations in the newly proposed model are integrated using the explicit substepping stress point algorithm for simplicity [17].

3. CALIBRATION OF SOIL PARAMETERS

Eleven parameters are defined in the proposed double surface model. Five of them (λ, κ, G_{ref}, N_0 and M) are similar to those in the Cam-clay model and two parameters (Γ_0 and n) are adopted to control the shape of bounding surface. Three parameters (α_s, r_N and r_Γ) are used to consider the influence of temperature on soil behaviour. One more parameter (n_c) is newly introduced to control the accumulation rate of plastic strain with increasing number of cycles. Parameter n_c is calibrated based on measured soil response during the first two thermal cycles. Calibration procedures of the other ten parameters were reported by Zhou *et al.* [8] in detail. The values of model parameters for three different soils are determined and summarized in Table 1.

4. COMPARISON BETWEEN MEASURED AND COMPUTED THERMAL CYCLIC BEHAVIOUR

Figure 3 compares measured and computed responses of reconstituted Boom clay subjected to one thermal cycle at isotropic stress state. The experimental results was reported by Baldi *et al.* [18]. It is clear that with an overconsolidation raio (OCR) of 1 and 2, measured and computed soil responses are quite consistent. With an OCR of 6, the new model slightly overestimates the thermally induced contraction. The model capability of simulating soil response with a higher OCR could be improved by slightly increasing the value of the term $\bar{\rho}_2 / \rho$ in equation (9). Considering that the differences between the measured and computed results are much smaller compared to the differences induced by OCR effects, no further modification is made in the current model to keep equation (9) simple.

Di Donna *et al.* [14] measured cyclic thermal strains of a saturated intact silty clay at normally consolidated state by using a temperature-controlled oedometer. Figure 4 shows the measured and computed soil behaviour under cyclic heating and cooling. Computed soil plastic strains are fairly consistent with the measured results. Based on the data in this figure, the computed and measured relationships between plastic strains and number of thermal cycles are calculated and shown in Figure 5. Computed results by the cyclic model of Di Donna *et al.* [14] are shown in the figure for comparison. It is clear that the accuracies of the two models are comparable. Without defining a series of nesting surfaces with additional hardening and translation rules, the newly proposed model has the advantage over the model of Di Donna *et al.* [14] due to the simplicity.

Figure 6 shows measured and computed thermal strain of a saturated compacted silt with different OCRs. The experimental results was reported by Vega *et al.* [2] through a

temperature-controlled oedometer. It can be seen that at slightly overconsolidated state (i.e., OCR = 1 and 1.3), measured and computed plastic strain accumulations are quite consistent. At a higher OCR (i.e., 1.8 and 7.5), however, there is an obvious discrepancy between measured and computed thermal strains. This is likely because the thermal expansion and contraction of oedometer ring, which impose more significant influence on the measured soil strains at a higher OCR [2], is not considered in the proposed model.

The capability of the proposed model for simulating thermal cyclic behaviour (see Figures 4 through 6) can be explained by different hardening laws of the memory surface and bounding surface. As illustrated above, apart from soil temperature, the size of the memory surface and bounding surface is governed by the maximum stress experienced and the preconsolidation pressure, respectively. When a soil specimen is subjected to cyclic heating and cooling at a constant effective stress, the current stress does not exceed the maximum stress experienced. Hence, the memory surface remains unchanged under thermal cycles. On the contrary, the bounding surface would expand due to the accumulation of plastic volumetric strain. With an increasing number of thermal cycles, the distance between the two surfaces increases, resulting from an increase in the accumulated plastic volumetric strain but at a reduced rate until reaching a stable state. Hence, the values of $\bar{\rho}_2/\ \bar{\rho}_1$ and K_p increase (see equation (9)).

5. SUMMARY AND CONCLUSIONS

An elastoplastic model is newly developed to simulate soil behaviour under thermal cycles. The original bounding surface plasticity theory is modified by constructing double surfaces. The bounding surface and memory surface are governed by the preconsolidation pressure (a

function of plastic volumetric strain) and the maximum stress state, respectively. Due to different hardening laws of the two surfaces, thermal cyclic effects are captured by incorporating the double surface concept.

The proposed model is applied to simulate the behaviour of two soils subjected to thermal cycles. The plastic soil strain accumulates with an increase in number of thermal cycles, but at a decreasing rate, until stabilization. It is shown that measured and computed soil volume changes under thermal cycles are generally consistent.

ACKNOWLEDGEMENTS

The research grant 51509041 provided by the National Science Foundation of China is also gratefully acknowledged. In addition, the authors would like to thank the Research Grants Council (RGC) of the HKSAR for providing financial support through the grants 16209415, 16216116, 617213 and HKUST6/CRF/12R.

APPENDIX

Elasto-plasticity

The total strain increment is the sum of the elastic strain increment and plastic strain increment:

$$\begin{cases} d\varepsilon_v = d\varepsilon_v^e + d\varepsilon_v^p \\ d\varepsilon_s = d\varepsilon_s^e + d\varepsilon_s^p \end{cases} \tag{10}$$

$$de = (1+e)\left(d\varepsilon_v + \alpha_s\, dT\right) \tag{11}$$

Elastic moduli

The elastic moduli K and G_0 are expressed as functions of stress state and void ratio as

follows:

$$K = \frac{(1+e)\,p'}{\kappa} \tag{12}$$

$$G_0 = G_{ref}\,(1+e)^{-3}\left(\frac{p'}{p_{atm}}\right)^{0.5} \tag{13}$$

Normal compression line (NCL)

The NCLs at two different temperatures are assumed to be parallel. With an increase in soil temperature, the NCL shifts to a smaller void ratio.

$$\upsilon = N(T) - \lambda \ln(\frac{p'}{p_{atm}}) \tag{14}$$

$$N(T) = N_0 - r_N (T - T_0) \tag{15}$$

Critical state line (CSL)

Similar to NCLs, the CSLs at different temperatures are modelled as parallel straight lines in the *v*-ln*p*' plane.

$$\upsilon = \Gamma(T) - \omega \ln(\frac{p'}{p_{atm}}) \tag{16}$$

$$\Gamma(T) = \Gamma_0 - r_\Gamma (T - T_0) \tag{17}$$

$$q = M\ p' \tag{18}$$

Bounding surface

Thermal effects on p0 and pm can be derived from temperature-dependent NCL [16]：

$$r = \exp\left[\frac{(N_0 - \Gamma_0) - (r_N - r_\Gamma)(T - T_0)}{\lambda - \kappa}\right] \tag{19}$$

$$p_0 = p_0^* \exp[-\beta(T - T_0)] \tag{20}$$

$$p_m = p_m^* \exp\left[-\beta\left(T - T_0\right)\right] \tag{21}$$

$$\beta = \frac{r_N}{\lambda - \kappa} \tag{22}$$

$$dp_0 = p_0\left(\frac{\upsilon}{\lambda - \kappa} d\varepsilon_v^p - \beta dT\right) \tag{23}$$

Flow rule

A non-associated flow rule is used in the proposed model:

$$D_s = \left(\frac{\left(M\,\rho/\bar{\rho}\right)^2 - \eta^2}{2\eta}\right) \tag{24}$$

Hardening law

The condition of consistency is expressed as

$$\frac{\partial F}{\partial p'} dp' + \frac{\partial F}{\partial q} dq + \frac{\partial F}{\partial r}\frac{\partial r}{\partial T} dT + \frac{\partial F}{\partial p_0}\frac{\partial p_0}{\partial T} dT + \frac{\partial F}{\partial p_0}\frac{\partial p_0}{\partial \varepsilon_v^p} D_s \Lambda_s = 0 \tag{25}$$

The value of each term in equation (25) can be calculated from equation (1):

$$\frac{\partial F}{\partial p'} = -n\left(\frac{q}{M}\right)^n p'^{-n-1} + \frac{1}{p' \ln r} \tag{26}$$

$$\frac{\partial F}{\partial q} = n\left(\frac{1}{Mp'}\right)^n q^{n-1} \tag{27}$$

$$\frac{\partial F}{\partial r}\frac{\partial r}{\partial T} = \frac{\ln\left[p' / p_0(T)\right]}{\left(\ln r\right)^2}\frac{\left(r_N - r_\Gamma\right)}{\lambda - \kappa} \tag{28}$$

$$\frac{\partial F}{\partial p_0}\frac{\partial p_0}{\partial T} = \frac{\beta}{\ln r} \tag{29}$$

$$K_p = -\frac{\partial F}{\partial p_0}\frac{\partial p_0}{\partial \varepsilon_v^p} D_s \tag{30}$$

$$K_p = \frac{\upsilon}{(\lambda - \kappa)\ln r} \frac{\left(M^2 - \eta^2\right)}{2\eta} \tag{31}$$

REFERENCES

1. Gens A. Soil-environment interactions in geotechnical engineering. *Géotechnique* 2010, **60**: 3-74.

2. Vega A, McCartney JS. Cyclic heating effects on thermal volume change of silt. *Environmental Geotechnics* 2014, **2**: 257-268.

3. Hueckel T, Borsetto M. Thermoplasticity of saturated soils and shales: constitutive equations. *Journal of Geotechnical Engineering, ASCE* 1990, **116**: 1765-1777.

4. Cui YJ, Sultan N, Delage P. A thermomechanical model for saturated clays. *Canadian Geotechnical Journal* 2000, **37**: 607-620.

5. Abuel-Naga H, Bergado D, Bouazza A, Pender M. Thermomechanical model for saturated clays. *Géotechnique* 2009, **59**: 273-278.

6. Laloui L, François B. ACMEG-T: Soil thermoplasticity model. *Journal of Engineering Mechanics, ASCE* 2009, **135**: 932-944.

7. Hong PY, Pereira JM, Tang AM, Cui YJ. On some advanced thermo‐mechanical models for saturated clays. *International Journal for Numerical and Analytical Methods in Geomechanics* 2013, **37**: 2952-2971.

8. Zhou C, Ng CWW. A thermo-mechanical model for saturated soil at small and large strains. *Canadian Geotechnical Journal* 2015, **52**: 1101-1110.

9. Masin D, Khalili N. A thermo‐mechanical model for variably saturated soils based on hypoplasticity. *International Journal for Numerical and Analytical Methods in*

Geomechanics 2012, **36**: 1461-1485.

10. Yao YP, Zhou AN. Non-isothermal unified hardening model: a thermo-elasto-plastic model for clays. *Geotechnique* 2013, **63**: 1328-1345.
11. Hong P, Pereira JM, Cui YJ, Tang AM. A two‐surface thermomechanical model for saturated clays. *International Journal for Numerical and Analytical Methods in Geomechanics* 2016, **40**: 1059-1080.
12. Semnani SJ, White JA, Borja RI. Thermoplasticity and strain localization in transversely isotropic materials based on anisotropic critical state plasticity. *International Journal for Numerical and Analytical Methods in Geomechanics* 2016, **40**: 2423-2449.
13. Xiong Y, Ye G, Zhu H, Zhang S, Zhang F. Thermo-elastoplastic constitutive model for unsaturated soils. *Acta Geotechnica* 2016, **11**: 1287-1302.
14. Di Donna A, Laloui L. Response of soil subjected to thermal cyclic loading: experimental and constitutive study. *Engineering Geology* 2015, **190**: 65-76.
15. Dafalias YF. Bounding surface plasticity. I: Mathematical foundation and hypoplasticity. *Journal of Engineering Mechanics, ASCE* 1986, **112**: 966-987.
16. Zhou C, Ng CWW. A thermomechanical model for saturated soil at small and large strains. *Canadian Geotechnical Journal* 2015, **52**: 1101-1110.
17. Potts DM, Zdravkovic L, Zdravković L. *Finite element analysis in geotechnical engineering: application*edn, vol. 2: Thomas Telford, 2001.
18. Baldi G, Hueckel T, Peano A, Pellegrini R. Developments in modelling of thermo-hydro-mechanical behaviour of Boom clay and clay-based buffer materials, vols 1

and 2, EUR13365/1 and 13365/2. *Luxembourg: Commission of European Communities* 1991.

NOTATION

D_s	soil dilatancy
$G_{0,}$ G_{ref}	elastic shear moduli and elastic shear modulus at a reference state
K	bulk modulus
K_p	plastic modulus
M	stress ratio (q/p') at the critical sate
N, N_0	intercept of NCL, value of N at reference temperature
T, T_0	temperature and reference temperature
$d\varepsilon_v$, $d\varepsilon_v^e$, $d\varepsilon_v^p$	incremental volumetric strain: total, elastic and plastic
$d\varepsilon_s$, $d\varepsilon_s^e$, $d\varepsilon_s^p$	incremental shear strain: total, elastic and plastic
e	void ratio
n	soil parameter describing bounding surface shape
p'	mean effective stress
p_0, p_{0*}	preconsolidation pressure and the value of p_0 at a reference temperature
p_m, p_{m*}	the maximum stress experienced and the value of p_0 at a reference temperature
p_{atm}	atmospheric pressure (101 kPa)
q	deviator stress
r_N, r_Γ	soil parameters describing thermal effects on intercepts of NCL and CSL
Γ,Γ_0	intercept of CSL, value of Γ_0 at reference temperature
Λ_s	loading index
α_s	thermal expansion coefficient of soil skeleton
η	stress ratio defined as q/p'
κ	slope of unloading and reloading lines in the υ-ln$p$' plane
λ	slope of NCL
ρ, $\bar{\rho}_1$, $\bar{\rho}_2$	Euclidian distance with respective to shearing
υ	specific volume

TABLES AND FIGURES

List of tables

List of figures

Table 1. Summary of model parameters

Soil parameters		Reconstituted Boom clay [18]	Compacted silt [2]	Intact silty clay [14]
Isothermal behaviour	λ	0.18	0.14	0.34
	κ	0.05	0.01	0.05
	G_{ref}	NIL*	180 MPa	33 MPa
	N_0	1.95	1.8	1.70
	M	NIL*	1.3	0.82
	n	NIL*	1	1
	Γ_0	NIL*	NIL*	NIL*
Thermo-plasticity	r_N	4.7×10^{-4}	1×10^{-4}	1.5×10^{-4}
	r_Γ	NIL*	1×10^{-4}	1.5×10^{-4}
Thermo-elasticity	α_s	0.25×10^{-4}	0.1×10^{-4}	0.18×10^{-4}
Cyclic behaviour	n_c	NIL*	12	50

* This parameter is not necessary in simulating stress paths considered in this study.

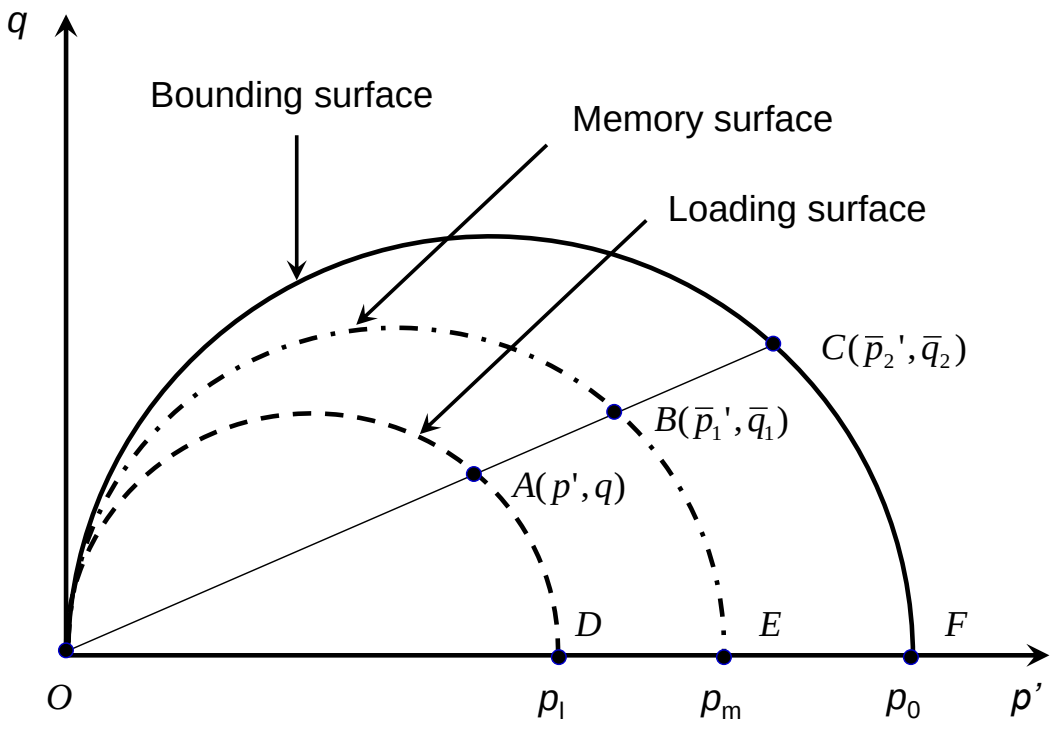

Figure 1. Double surfaces and loading surface in the *p*'- *q* plane

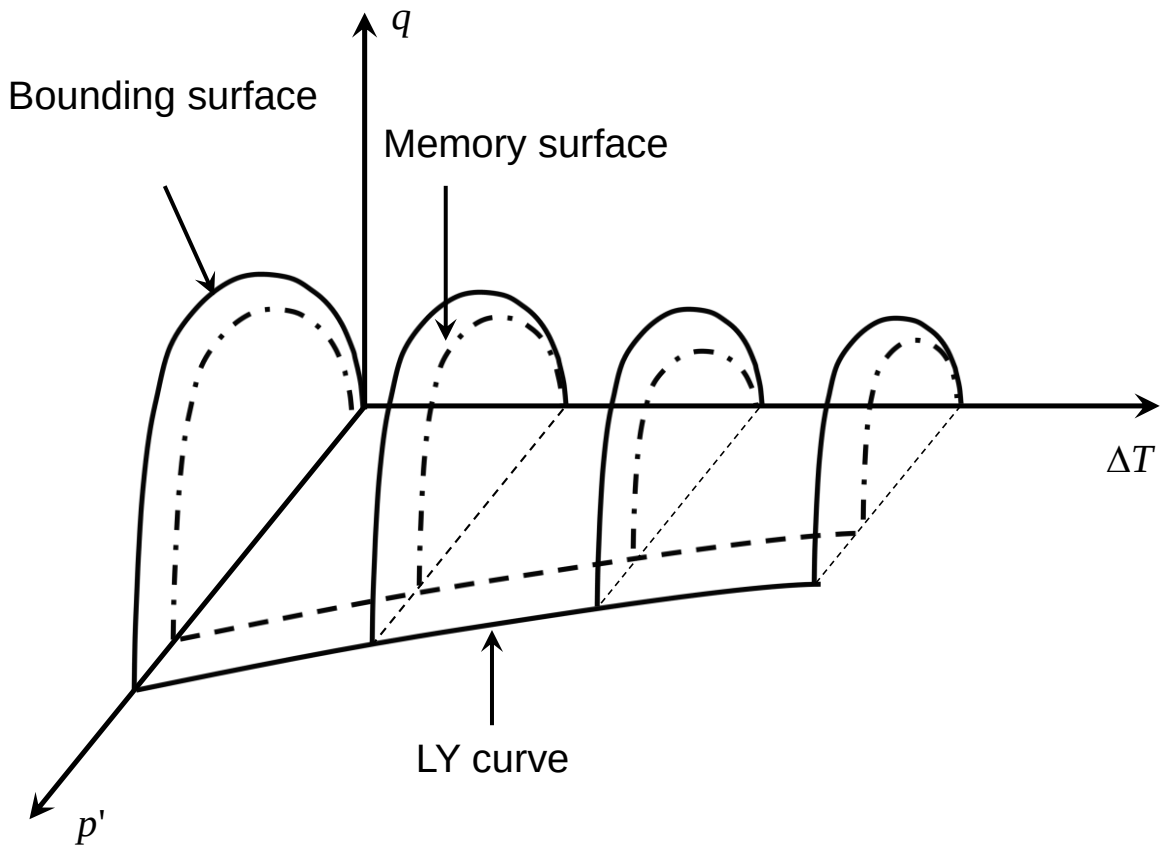

Figure 2. Double surfaces in the *p'*-*q*-Δ*T* space

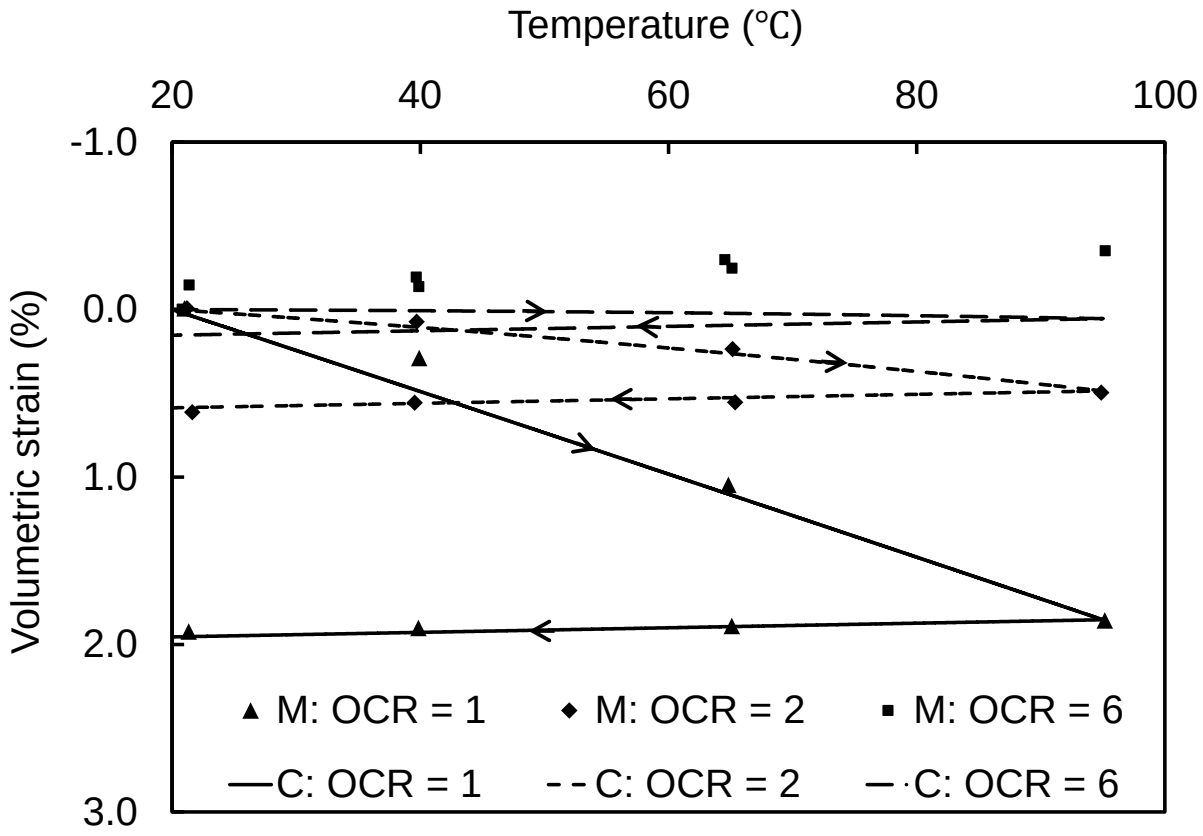

Figure 3. Comparisons between measured [18] and computed volume changes of reconstituted Boom clay during a heating and cooling cycle

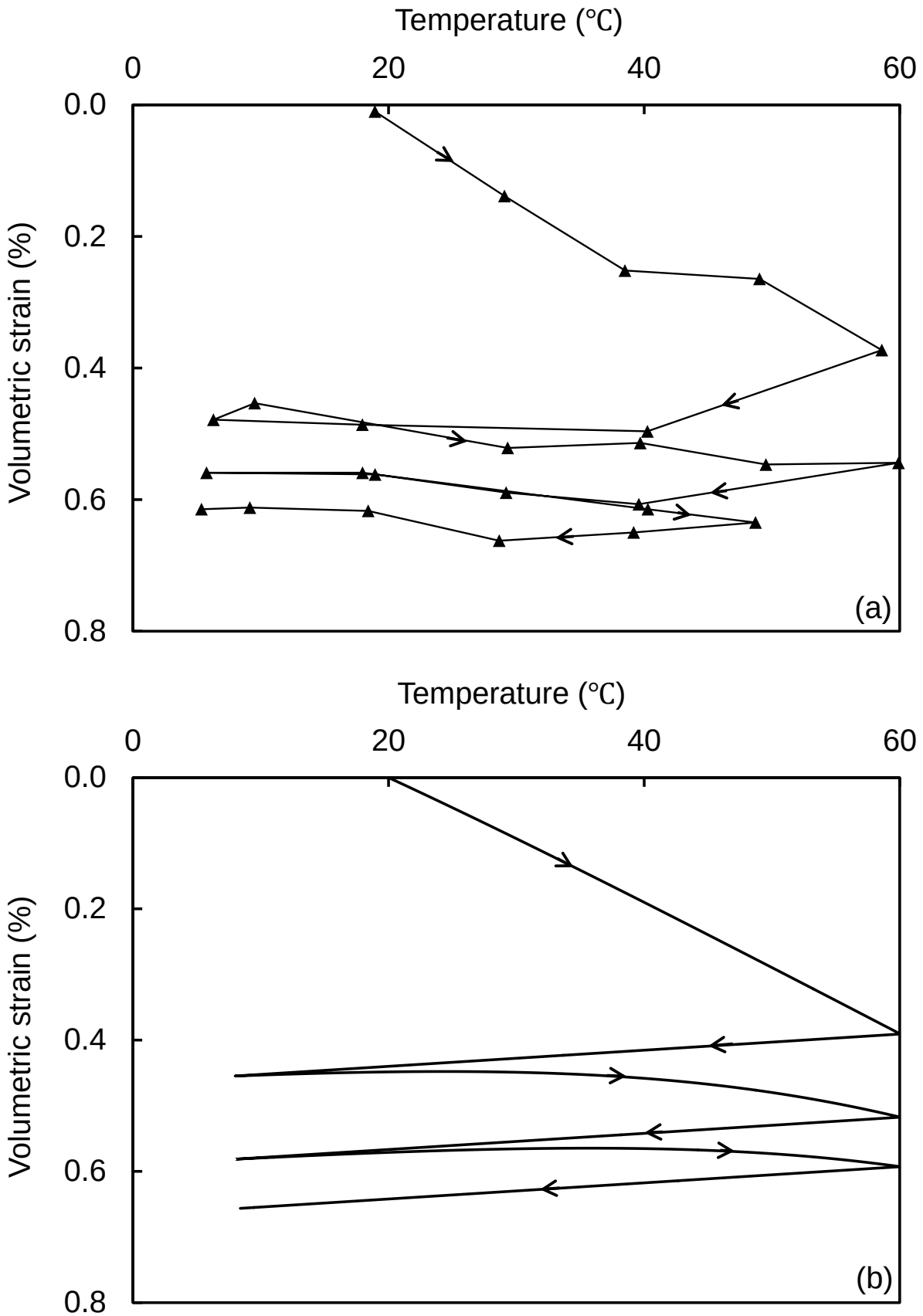

Figure 4. Thermal responses of an intact normally consolidated silty clay: (a) Measured by Di Donna & Laloui [14]; (b) Computed by using the proposed model

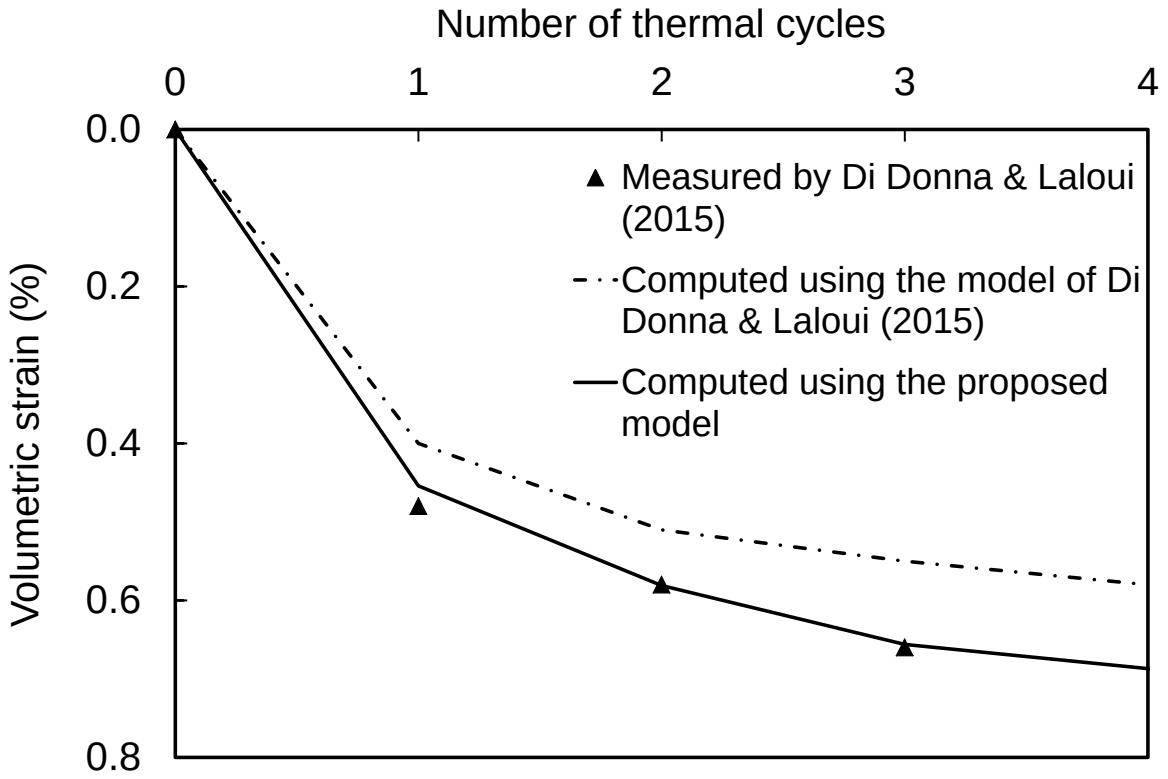

Figure 5. Comparisons between measured (M) [2] and computed (C) plastic strain accumulation of an intact normally consolidated silty clay under thermal cycles

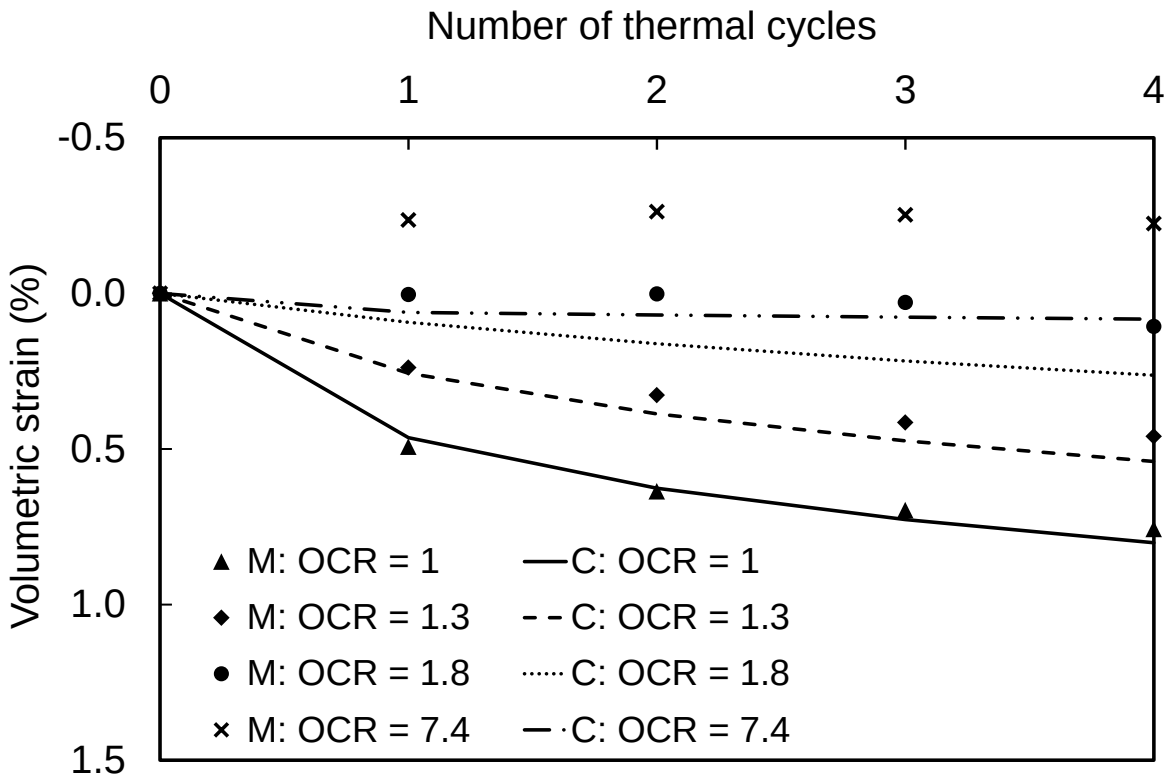

Figure 6. Comparisons between measured (M) [2]and computed (C) responses of compacted silt under thermal cycles in the temperature range of 18 to 91°C